



Reduced Field of View APT Imaging of Rectum (RAPTOR) at 3T MRI Scanner*

CHAI Xu-Bin^{1,2,3,6}, WANG Yi⁵, HE Zi-Jun³, LIU Ai-Hua^{3**}, XUE Rong^{1,2,4**}

¹State Key Laboratory of Brain and Cognitive Science, Institute of Biophysics, Chinese Academy of Sciences, Beijing 100101, China;

²University of Chinese Academy of Sciences, Beijing 100049, China;

³Beijing Neurosurgical Institute, Beijing Tiantan Hospital, Capital Medical University, Beijing 100070, China;

⁴Beijing Institute of Brain Disorders, Capital Medical University, Beijing 100069, China;

⁵Public Health Science and Engineering College, Tianjin University of Traditional Chinese Medicine, Tianjin 301617, China;

⁶Department of Biomedical Engineering, School of Medicine, Tsinghua University, Beijing 100084, China)

Abstract Objective The chemical exchange saturation transfer (CEST) technique has become a valuable tool in diagnosing metabolic changes associated with cerebral and systemic diseases, leveraging the calculation of compounds with exchangeable protons in proximity to water molecules. Specifically, the amide proton transfer (APT) CEST technique has shown promise in diagnosing cerebral strokes and tumors by comparing altered endogenous proteins or peptides with normal tissues. Reduced field of view (rFOV) imaging technology has been widely used in the diagnosis of small organ lesions in the body. In this study, we aim to apply the rFOV imaging to identify CEST signals in the rectum, investigating the potential utility of rFOV technique in clinical diagnosis of rectal diseases and providing metabolic insights for chemoradiotherapy. **Methods** MRI images of eleven healthy volunteers were acquired using transverse Full_FOV and rFOV CEST imaging on a 3T scanner. The resolution was set at $2.5 \times 2.5 \times 6$ mm³ and $1.5 \times 1.5 \times 6$ mm³ for Full_FOV or the rFOV method. Saturation powers of 0.7 μ T and 2 μ T were applied. For the 2 μ T saturation, MTR_{asym} at ± 3.5 ppm was employed, while for 0.7 μ T saturation, Lorentzian difference was used for CEST quantification of the contrast maps and curves. **Results** The rFOV method has the advantage of halving the scan time while maintaining the same contrast as the Full_FOV method. When compared to Full_FOV methods, rFOV methods exhibited nearly identical Z_{spec} and very similar MTR_{asym} curves. Additionally, rFOV with a 1.5 mm \times 1.5 mm in-plane resolution could be achieved in approximately 3 min. rFOV method displayed better structural details for the entire rectum, including CEST contrast maps and quantitative curves. **Conclusion** CEST MRI proves valuable in diagnosing rectal diseases, and employing the rFOV technique could provide higher spatial and temporal resolution. CEST MRI should be the preferred choice for offering improved diagnostic capabilities with its potential for rectal disease diagnosis.

Key words chemical exchange saturation transfer (CEST), reduced field of view (rFOV), full field of view (Full_FOV), rectum

DOI: 10.16476/j.pibb.2023.0461

Rectum cancer is the third most common cancer in men and the second most common in women^[1]. The higher incidence and lower mortality rate more happened in the developed countries especially caused by the improved diagnosis equipment and skills. Magnetic resonance imaging (MRI) has been used in diagnosis of rectal cancer in the MERCURY experience in eleven European clinics in multidisciplinary approach and proved the MRI could provide the basis for chemoradiotherapy and predict circumferential resection margin (CRM) status. The

* This work was supported by grants from Science and Technology Innovation 2030 (2022ZD0211901), National Key Research and Development Program of China (2020AAA0105601, 2019YFA070710 3), and Basic Frontier Science Research Program From 0 to 1 Original Innovation Project of Chinese Academy of Sciences (ZDBS-LY-SM028).

** Corresponding author.

LIU Ai-Hua. Tel: 86-10-67016611, E-mail: liuaihuadoctor@163.com

XUE Rong. Tel: 86-10-64888462, E-mail: rxue@ibp.ac.cn

Received: November 21, 2023 Accepted: February 23, 2024

role of MRI mainly focus on the assessment of local grading of rectum cancer, the selection of patients for the treatment of neoadjuvant chemoradiotherapy (CRT), help for formulate the surgery plan, monitor the tumor regression and evaluate therapeutic effects of the surgery operation or CRT^[2]. MRI has been widely used in diagnosis of the rectum cancer for the non-invasive and high-contrast of tissues with accurate imaging modality for local staging, while computed tomography (CT) and positron emission tomography (PET)/CT are more useful in detecting distant recurrence of the rectum cancer^[3]. Although the anatomical MRI images could provide high-contrast and high-resolution images^[4], it is hard to determine the grade of rectum cancer in metabolic aspect.

Magnetization transfer (MT) imaging method had been used to detect the intestinal fibrosis in an animal model of the Crohn disease^[5]. In this research, the authors proved that the MT ratio was higher in the Crohn disease rats than the control animals and could help to monitor the changes in fibrosis and the natural history of the Crohn disease. However, they haven't proven what were the specific substance which brought the MT effect and the results had been affected by the artifacts caused by the bowel movements or breath severely.

Chemical exchange saturation transfer (CEST) imaging is a promising molecular MRI technique and has been used in the rectal diseases^[6]. By calculating the average amide proton transfer imaging (APT) signal intensity (SI), we could predict tumor grade in rectal cancer groups^[7]. APT imaging can also predict the tumor response to neoadjuvant chemotherapy (NAC) in rectal cancer patients^[8]. However, when using the conventional Full-FOV method for acquisition, there is a poor signal-to-noise ratio and is easily affected by artifacts caused by intestinal peristalsis. The reduced-field-of-view (rFOV) technique had shown its superiority in imaging small-sized organs, for shortening scan time, increasing resolution and reducing artifacts caused by field inhomogeneity and motion^[9-10]. rFOV technique uses the 2D spatially selective excitation pulses to excite a small inner volume in the phase-encoding direction and the phase-encoding steps should be reduced in large scale^[11-12]. rFOV would improve accuracy of measurements while compare with the Full_FOV

sequence on the same scan duration^[13]. Liu *et al.*^[9, 14] has used the rFOV method in the human lumbar intervertebral discs and the rFOV method showed superior reproducibility and got more reliable results.

In this study, we examined the performance of the rFOV readout technique in the rectum tissue of eleven healthy volunteers in comparison with the Full_FOV CEST method on a 3T clinical scanner. We use two different B₁ (0.7 μ T and 2 μ T) and two different reduction degrees on the phase-readout direction (60 mm and 90 mm), to receive the CEST quantification of the contrast maps and the curves of MTR_{asym} at ± 3.5 ppm for 2 μ T saturation and the Lorentzian difference(LD) results in 0.7 μ T saturation.

1 Materials and methods

1.1 Healthy subjects

Eleven healthy volunteers (male, mean age 40.6 \pm 9.5 years) with no symptoms caused by rectum diseases were recruited at Tsinghua University. The research was permitted by the Medical Committee of Science and Technology Ethics Committee of Tsinghua University (ID: THU01-20230104) and informed consent was received from all of the volunteers.

1.2 MRI protocol

Eleven healthy volunteers underwent rectum MR examination with written informed consent signed before participation. MR scans were performed on a 3T scanner (Ingenia CX 3.0T; Philips Medical Systems, Best, the Netherlands), using a 16-channel torso coil and a 12-channel posterior coil as the receivers. A transverse plane crossing the rectum center was chosen for both Full_FOV readout and the rFOV readout. The MRI protocol includes the T1-weighted, T2-weighted and APT sequences with the of the Full_FOV and the rFOV technique which were performed after the localizer. The acquisition parameters of Full_FOV CEST scans with the single-shot spin-echo Turbo-Spin-Echo (TSE) sequence were: FOV=230 \times 320 mm², slices=1, thickness=6 mm, TR=5 600 ms, TE=7 ms, resolution=2.5 \times 2.5 \times 6 mm³, two sets of rFOV were acquired, with FOV of 230 \times 90 mm² and 230 \times 60 mm², in-plane resolution of 2.5 \times 2.5 \times 6 mm³ (rFOV_2.5 mm) and 1.5 \times 1.5 \times 6 mm³ (rFOV_1.5mm) respectively. The rest parameters of all datasets are shown in Table 1.

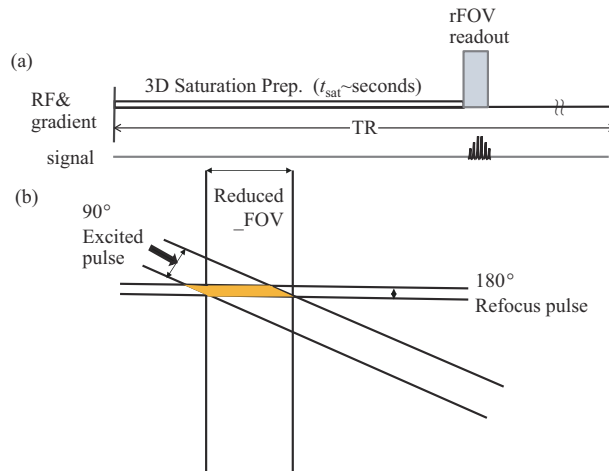
Table 1 Parameters of the Full_FOV and rFOV APT images of the healthy volunteers

| Sequence type | B1/ μ T | Voxel_size/ mm^3 | FOV/ mm^2 | Total scan time |
|---------------|-------------|-----------------------------|--------------------|-----------------|
| Full_FOV | 2 | 2.5 \times 2.5 \times 6 | 230 \times 320 | 03:38 |
| rFOV_2.5 mm | | 2.5 \times 2.5 \times 6 | 230 \times 90 | 01:52 |
| rFOV_1.5 mm | | 1.5 \times 1.5 \times 6 | 230 \times 60 | 01:52 |
| Full_FOV | 0.7 | 2.5 \times 2.5 \times 6 | 230 \times 320 | 06:15 |
| rFOV_2.5 mm | | 2.5 \times 2.5 \times 6 | 230 \times 90 | 03:10 |
| rFOV_1.5 mm | | 1.5 \times 1.5 \times 6 | 230 \times 60 | 03:10 |

1.3 Pulse sequence

CEST image was achieved by using an adjusted sequence based on the APT patch with TSE readouts, in combination with Philips rFOV technique. Briefly, after a 2-second long off-resonance saturation preparation, rFOV only read signal selectively at the crossing section of a 90 deg excitation slab and a 180

deg refocus slab that had an angle in between (Figure 1). Two series of CEST Z_{spec} data were acquired, one with saturation power of 0.7 μ T and 33 offsets distributed from -10 ppm to +10 ppm, another with 2 μ T saturation and 19 offsets from -4.5 ppm to +4.5 ppm with 0.5 ppm step size, one image without saturation (S_0).

**Fig. 1** Schematic diagram of the reduced field of view imaging sequence

(a) The continuous wave (CW) readout method for CEST imaging. (b) The rFOV method employed in this research.

1.4 Data process

All data underwent processing using custom-written MATLAB scripts, utilizing MTRasym at 3.5 ppm for CEST quantification. Moreover, for 0.7 μ T saturation, the Lorentzian difference was employed for both contrast maps and curves. The magnetization transfer ratio (MTR) asymmetry at 3.5 ppm was calculated as follows:

$$\text{MTRasym}(3.5 \text{ ppm}) = \frac{\text{Ssat}(-3.5 \text{ ppm}) - \text{Ssat}(3.5 \text{ ppm})}{S_0} \quad (1)$$

The terms “Ssat” and “ S_0 ” represent the water signal acquired with and without the pre-saturation

RF pulses, respectively. The Lorentzian difference was defined as follows:

$$LD(\Delta\omega) = \frac{A}{\pi \left[1 + \frac{\omega_1 - \omega}{\sigma} \right]^2} - Z_{\text{spec}} \quad (2)$$

Where ω_1 represents the frequency offsets from the water resonance; A , ω , and σ denote the amplitude, frequency offset, and linewidth of the CEST peak for the proton pool, respectively.

2 Results

This presentation showcases CEST images and spectra for a saturation B1 strength of 2 μ T. The

layout includes comparisons of three acquisition sequences (Full_FOV, rFOV_2.5 mm, and rFOV_1.5 mm) with specific focus on S0 images, overlap results with Z_spec images at Z(-3.5 ppm), Z(3.5 ppm), and MTRAsym(3.5 ppm). Note that pseudo-colored images only display the reduced rectum region for better comparison (Figure 2). The contrast maps and the quantitative curves of the whole rectum region, using a 2 μ T saturation power employed by the standard APTw protocol. It proved that rFOV could reduce the scan time by half while kept the same contrast as the Full_FOV method. Furthermore, a smaller FOV with a 1.5 mm \times 1.5 mm in-plane resolution could be completed within 3 min and displayed better structure details of the rectum (Figure

2). Furthermore, compared with Full_FOV methods, rFOV methods displayed almost identical Z_spec and very closed MTRAsym curves, that averaged for the entire rectum.

The application of CEST sequences (LD_APT, LD_Amine, LD_G-amine, LD_PCr, and LD_NOE) with a B1 strength of 0.7 μ T for rectum imaging showed the Z_spec results highlight distinct signal changes within the specified ppm range, and the rFOV results are approximately consistent with the Full_FOV method while only cost half of the time used by the Full_FOV. Additionally, LD results across all three methods indicate that rFOV images consistently exhibit more stable signals (Figure 3).

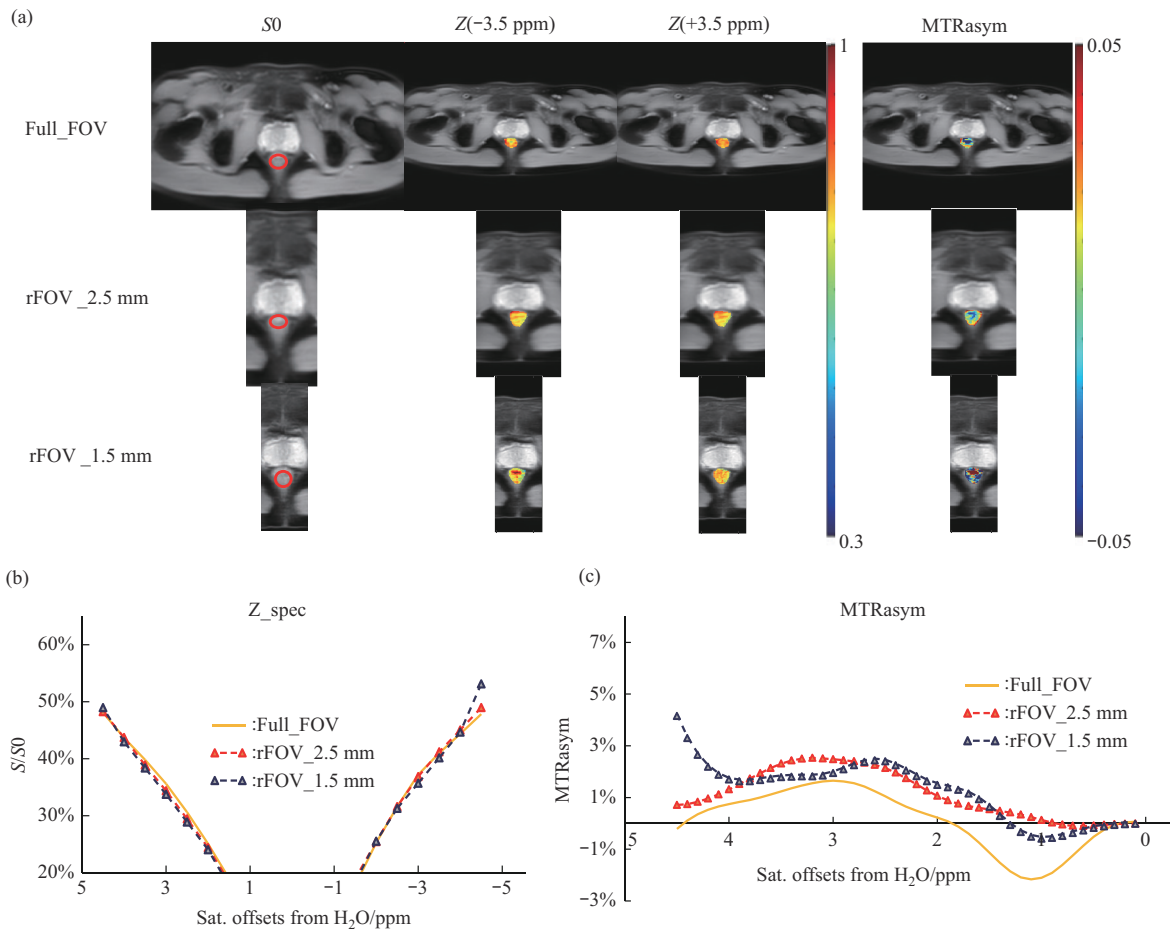


Fig. 2 CEST images and spectra for saturation B1 strength of 2 μ T

(a) CEST images for three different acquisition sequences, Full_FOV (row 1), rFOV_2.5 mm (row 2) and rFOV_1.5 mm (row 3). From left to right, S0 with the actual acquired size, the overlap results between the S0 and the Z_spec image at 3.5 ppm (Z(-3.5 ppm)), Z(3.5 ppm) and MTRAsym (3.5 ppm). Noted that for the pseudo-colored images only reduced rectum region is displayed for comparison. (b, c) The averaged Z_spec and MTRAsym curved of the entire rectum, Z_spec showed the good consistency among the three methods. The rFOV methods stand for higher MTRAsym results while compare with the Full_FOV method.

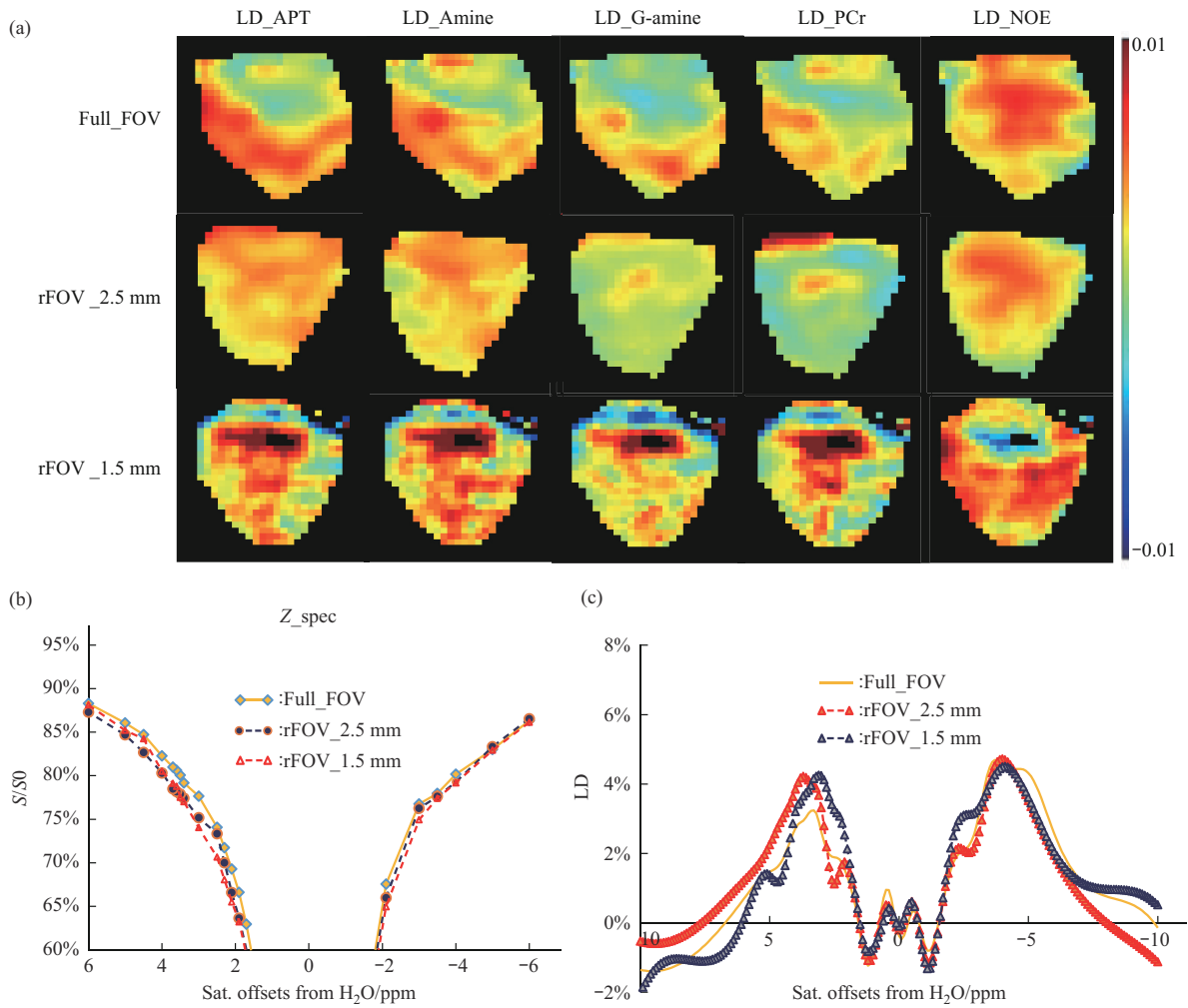


Fig. 3 The Z_{spec} and LD results of the three methods

(a) CEST sequences (LD_APT, LD_Amine, LD_G-amine, LD_PCr, and LD_NOE) with a B₁ strength of 0.7 μ T for rectum imaging. (b) Z_{spec} results of the three sequences shows the obviously signal changed in the ± 3.5 ppm, and the rFOV results are approximately consistent with the Full_FOV method while only cost half of the time used by the Full_FOV. (c) LD results of the three methods shows the rFOV images indicated the signals are more stable.

3 Discussion

On the Philips 3T Ingenia MRI system platform, a multi-saturation conditional dynamic saturation reading sequence has been developed. The parameters have been optimized for rectum scans in transverse plane imaging. The widely used APT sequences, the quantification, specificity, and contrast-to-noise ratio of MRI images have seen substantial improvements on a large scale. By using a small B₁ (B₁=0.7 μ T), the Z_{spec} can be obtained within 2 min. Amide proton signals, amine proton signals from protein or peptide components, and even the NOE signal reflecting lipid composition can be quantitatively separated by

Lorentz difference. The rFOV technique, at the same resolution, expends half the time of the Full_FOV method. Traditional Full_FOV imaging scans are time-consuming, and they are susceptible to the impact of intestinal peristalsis and respiratory movements, resulting in noticeable motion artifacts. In this study, we opted for two distinct small field of view imaging sizes, namely 90 mm and 60 mm. This choice was primarily guided by the average width of the human pelvic cavity and the specific volume of the rectum. The actual FOV window size for MRI scans is determined based on the real volume of small pelvic organs, aiming to enhance the clinical applicability of the approach.

Furthermore, a reduced-FOV CEST imaging technique for the rectum has been developed and evaluated. This method utilizes 3D saturation pulse excitation, and a classic reduced field of view reading technology is employed for readout. Specifically, in gradient selection at different refocusing angles of 90 degrees and 180 degrees using fast spin echo sequences. This approach, especially beneficial for scanning small pelvic organs like the rectum, results in reduced scanning time and improved spatial resolution. The image consistency between the reduced field of view CEST spectrum and map and the full field of view has been verified at different saturation intensities. The reduced field of view allows for higher spatial resolution and fewer motion artifacts caused by bowel movements or breaths.

Some limitations exist in this study. Firstly, it was conducted in a single institution with not enough number of volunteers. More healthy volunteers and patients with rectum cancer should be involved to further enhance its clinical value. The Z-spectrum and MTRasym curves, which capture the essential characteristics of rectal diseases, are not thoroughly comprehended. The code for processing the data remains unpublished and is currently undergoing further refinement. Phantom tests should be conducted to optimize the parameters of the RF pulses and B1 value. Saturation time and B1 strength need further refinement for better CEST signals. B1-correction is crucial for evaluating CEST images, especially at high field strengths with strong B1-inhomogeneities^[15]. Secondly, considering that many reported papers use the DWI sequence to diagnose rectum diseases, we should add the DWI sequence as a better contrast method to verify CEST results.

4 Conclusion

rFOV sequence could offer both superior signal quality and efficiency in rectum imaging. The anatomical details of the rectum have been enhanced with this method. It is recommended for clinical use as the standard sequence due to its potential to discern differences in metastatic aspects of the target tissues. Moreover, it improves doctors' diagnostic capabilities, enabling them to identify earlier changes that may not have been confirmed by the Full_FOV methods.

Acknowledgement The authors are grateful to our colleagues, Drs. ZUO Zhen-Tao and ZHANG Zi-Hao from State Key Laboratory of Brain and Cognitive Science, Institute of Biophysics, Chinese Academy of Sciences for their valuable technical suggestions, and Ms. HU Kun from State Key Laboratory of Brain and Cognitive Science, Institute of Biophysics, Chinese Academy of Sciences for helping in finding healthy volunteers.

References

- [1] Ferlay J, Soerjomataram I, Dikshit R, *et al.* Cancer incidence and mortality worldwide: sources, methods and major patterns in GLOBOCAN 2012. *Int J Cancer*, 2015, **136**(5): E359-E386
- [2] Sinaei M, Swallow C, Milot L, *et al.* Patterns and signal intensity characteristics of pelvic recurrence of rectal cancer at MR imaging. *Radiographics*, 2013, **33**(5): E171-E187
- [3] Horvat N, Carlos Tavares Rocha C, Clemente Oliveira B, *et al.* MRI of rectal cancer: tumor staging, imaging techniques, and management. *Radiographics*, 2019, **39**(2): 367-387
- [4] Shihab O C, Heald R J, Rullier E, *et al.* Defining the surgical planes on MRI improves surgery for cancer of the low rectum. *Lancet Oncol*, 2009, **10**(12): 1207-1211
- [5] Adler J, Swanson S D, Schmiedlin-Ren P, *et al.* Magnetization transfer helps detect intestinal fibrosis in an animal model of Crohn disease. *Radiology*, 2011, **259**(1): 127-135
- [6] Gao T, Zou C, Li Y, *et al.* A brief history and future prospects of CEST MRI in clinical non-brain tumor imaging. *Int J Mol Sci*, 2021, **22**(21): 11559
- [7] Nishie A, Takayama Y, Asayama Y, *et al.* Amide proton transfer imaging can predict tumor grade in rectal cancer. *Magn Reson Imaging*, 2018, **51**: 96-103
- [8] Nishie A, Asayama Y, Ishigami K, *et al.* Amide proton transfer imaging to predict tumor response to neoadjuvant chemotherapy in locally advanced rectal cancer. *J Gastroenterol Hepatol*, 2019, **34**(1): 140-146
- [9] Liu Q, Jin N, Fan Z, *et al.* Reliable chemical exchange saturation transfer imaging of human lumbar intervertebral discs using reduced-field-of-view turbo spin echo at 3.0 T. *NMR Biomed*, 2013, **26**(12): 1672-1679
- [10] Zhang Y, Holmes J, Rabanillo I, *et al.* Quantitative diffusion MRI using reduced field-of-view and multi-shot acquisition techniques: validation in phantoms and prostate imaging. *Magn Reson Imaging*, 2018, **51**: 173-181
- [11] Tamada T, Ream J M, Doshi A M, *et al.* Reduced field-of-view diffusion-weighted magnetic resonance imaging of the prostate at 3 tesla: comparison with standard echo-planar imaging technique for image quality and tumor assessment. *J Comput Assist Tomogr*,

- 2017, **41**(6):949-956
- [12] Rosenkrantz A B, Chandarana H, Pfeuffer J, *et al.* Zoomed echo-planar imaging using parallel transmission: impact on image quality of diffusion-weighted imaging of the prostate at 3T. *Abdom Imaging*, 2015, **40**(1): 120-126
- [13] Samson R S, Lévy S, Schneider T, *et al.* ZOOM or non-ZOOM? Assessing spinal cord diffusion tensor imaging protocols for multi-centre studies. *PLoS One*, 2016, **11**(5): e0155557
- [14] Lu Y, Hatzoglou V, Banerjee S, *et al.* Repeatability investigation of reduced field-of-view diffusion-weighted magnetic resonance imaging on thyroid glands. *J Comput Assist Tomogr*, 2015, **39**(3): 334-339
- [15] Windschuh J, Zaiss M, Meissner J E, *et al.* Correction of B1-inhomogeneities for relaxation-compensated CEST imaging at 7 T. *NMR Biomed*, 2015, **28**(5): 529-537

3T磁共振直肠小视野APT成像*

柴旭斌^{1,2,3,6)} 王翌⁵⁾ 何子骏³⁾ 刘爱华^{3)**} 薛蓉^{1,2,4)**}

⁽¹⁾ 中国科学院生物物理研究所, 脑与认知科学国家重点实验室, 北京 100101;

⁽²⁾ 中国科学院大学, 北京 100049;

⁽³⁾ 首都医科大学, 北京天坛医院, 北京市神经外科研究所, 北京 100070;

⁽⁴⁾ 首都医科大学, 北京脑重大疾病研究院, 北京 100069; ⁽⁵⁾ 天津中医药大学, 公共卫生与健康科学学院, 天津 301617;

⁽⁶⁾ 清华大学医学院生物医学工程系, 北京 100084)

摘要 目的 化学交换饱和和转移 (CEST) 成像技术已成为诊断与脑部和全身疾病代谢相关变化的有用工具, 通过计算与水分子相邻化合物的可交换质子的含量进行定量分析。具体而言, 酰胺质子转移 (APT) CEST 技术通过比较可交换的内源性蛋白质或肽的含量变化来区分正常组织与脑卒中和脑肿瘤组织。在体内的小器官病变诊断中, 小视野 (rFOV) 成像技术已被广泛应用, 本研究旨在应用 rFOV 成像技术来识别直肠中的 CEST 信号, 探讨 rFOV 成像技术在直肠疾病临床诊断中的潜在效用, 并为直肠疾病的放化疗提供代谢影像信息。**方法** 使用 3.0T 磁共振成像扫描仪对 11 名健康志愿者进行了横断面全视野 (Full_FOV) 和 rFOV CEST 成像。设置的分辨率分别为 $2.5 \times 2.5 \times 6 \text{ mm}^3$ 和 $1.5 \times 1.5 \times 6 \text{ mm}^3$ 。采用了 $0.7 \mu\text{T}$ 和 $2 \mu\text{T}$ 两种预饱和脉冲。rFOV 成像采用了 ZOOM 成像方法。对于 $2 \mu\text{T}$ 的饱和脉冲, 采用了 $\pm 3.5 \text{ ppm}$ 的 MTRasym 方法进行定量分析, 而对于 $0.7 \mu\text{T}$ 的饱和脉冲, 则采用 Lorentzian Difference 的方法来量化 CEST 的对比度图和曲线。**结果** 相较于 Full_FOV 成像, rFOV 方法可以在保持较好对比度的同时将扫描时间减半。与 Full_FOV 方法相比, rFOV 成像方法可以得出与 Full_FOV 方法几乎相同的 Z 谱和 MTRasym 曲线。此外, 以大约 3 min 的时间可以实现 $1.5 \text{ mm} \times 1.5 \text{ mm}$ 分辨率的 rFOV 成像。这种 rFOV 成像方法可以更好地显示出整个直肠的解剖细节, 包括 CEST 成像对比图及定量分析曲线。**结论** CEST MRI 在直肠疾病诊断方面具有较高价值, 采用 rFOV 技术可以提供更高的空间和时间分辨率。由于其在直肠疾病诊断方面的潜力, CEST MRI 可以作为临床诊断直肠疾病的首选。

关键词 化学交换饱和和转移成像, 小视野, 全视野, 直肠

中图分类号 R445.2

DOI: 10.16476/j.pibb.2023.0461

* 科技创新2030 (2022ZD0211901), 国家重点研发计划 (2020AAA0105601, 2019YFA0707103) 和中国科学院基础前沿科学计划从0到1原始创新项目 (ZDBS-LY-SM028) 资助。

** 通讯联系人。

刘爱华 Tel: 010-67016611, E-mail: liuaihuadoctor@163.com

薛蓉 Tel: 010-64888462, E-mail: rxue@ibp.ac.cn

收稿日期: 2023-11-21, 接受日期: 2024-02-23